

Fractional Calculus—A Different Approach to the Analysis of Viscoelastically Damped Structures

Ronald L. Bagley*

United States Air Force Academy, Colorado Springs, Colorado
and

Peter J. Torvik†

Air Force Institute of Technology, Wright-Patterson Air Force Base, Ohio

Fractional calculus is used to construct stress-strain relationships for viscoelastic materials. These relationships are used in the finite element analysis of viscoelastically damped structures and closed-form solutions to the equations of motion are found. The attractive feature of this approach is that very few empirical parameters are required to model the viscoelastic material and calculate the response of the structure for general loading conditions.

Nomenclature

$\{ \}, \{ \}^T$	= column vector, row vector
$\langle \rangle$	= argument of operator
$[]$	= square matrix
A	= bar area, example
A_s	= area of shear pad, example
b	= model parameter
c	= time-scaling factor, example
$[C]$	= damping matrix
D^α	= fractional derivative of order α
E	= bar modulus, example
$\{f(t)\}$	= column vector of applied forces
$\{F(s)\}$	= Laplace transform of force vector
$[K]$	= stiffness matrix
L	= bar length, example
$[M]$	= mass matrix
m_j	= modal constant
s	= Laplace parameter
t	= time
t_i	= thickness of shear pad, example
$\{x(t)\}$	= column vector of nodal displacement
$\{X(s)\}$	= transform of displacement vector
$\{\hat{x}(t)\}$	= column vector of displacements for impulsive loading
$\{\hat{X}(s)\}$	= transform of displacement vector for impulsive loading
α, β	= model parameters
$\epsilon(t)$	= strain history
$\epsilon^*(s), \epsilon^*(i\omega)$	= Laplace and Fourier transforms of the strain history
λ_n	= n th eigenvalue
$\mu^*(s), \mu^*(i\omega)$	= Laplace and Fourier transforms of the shear relaxation modulus
ρ	= bar density, example
$\sigma(t)$	= stress history
$\sigma^*(s), \sigma^*(i\omega)$	= Laplace and Fourier transforms of the stress history
τ	= dimensionless time, example; also, dummy variable

$\{\phi_n\}$	= n th mode shape
ω	= frequency
(\sim)	= associated with the expanded equations of motion

Introduction

THE successful determination of the responses of a viscoelastically damped structure to prescribed loading time histories hinges on the successful solution of two problems. The first problem is that of describing the viscoelastic material's mechanical properties in a mathematically rational manner that enhances the prospects of successfully attacking the second problem—solving the resulting equations of motion for the structure.

Fractional derivative stress-strain constitutive relationships for viscoelastic solids not only describe the mechanical properties of some materials, but lead to closed-form solutions of the finite element equations of motion for viscoelastically damped structures.¹ We will present the basic form of a fractional derivative model for a viscoelastic material and then outline construction and solution of the resulting finite element equations of motion.

Previous attempts to describe the mechanical properties of viscoelastic solids have suffered because the mathematical models describing the behavior of these materials have not been clearly linked to the physical principles involved. The engineer has been forced to adopt phenomenological (empirical) approaches to describe mechanical properties of these materials. Some of the more popular approaches are a complex constant as material modulus, numerical methods in the transform domain, and the standard linear viscoelastic model presented in textbooks.

The simplest of these approaches is using a complex constant as the material modulus. This approach is motivated by observing the relationship between sinusoidal stress and sinusoidal strain in viscoelastic materials. The strain lags the stress and the imaginary part of the complex constant adequately describes this phenomenon. The limitation of this approach is that it is restricted to sinusoidal motion of the material. Crandall has shown² that application of this method to the general motion of the material leads to serious mathematical problems.

The use of numerical methods in the transform domain to describe the frequency-dependent mechanical properties of viscoelastic materials is cumbersome at best. The major drawback is the substantial effort required to calculate numerically the transform inversion integral for every point in time at which the response of the structure is needed.

Presented as Paper 81-0484 at the AIAA/ASME/ASCE/AHS 22nd Structures, Structural Dynamics and Materials Conference, Atlanta, Ga., April 6-8, 1981; submitted April 15, 1981; revision received July 19, 1982. This paper is declared a work of the U. S. Government and therefore is in the public domain.

*Associate Professor, Department of Engineering Mechanics.

†Professor and Head, Department of Aeronautics and Astronautics. Associate Fellow AIAA.

The standard linear viscoelastic model, a series of derivatives acting on the stress fields related to a series of time derivatives on the strain fields

$$\sigma(t) + \sum_{m=1}^M b_m \frac{d^m \sigma(t)}{dt^m} = E_0 \epsilon(t) + \sum_{n=1}^N E_n \frac{d^n \epsilon(t)}{dt^n} \quad (1)$$

is also cumbersome to use. For viscoelastic materials having mechanical properties that are strongly frequency dependent over many decades of frequency, the number of time derivatives, M and N , in the series is large. Consequently the number of empirical parameters in the model is large. As a result, the model is time consuming to manipulate and, when put into the equations of motion, produces high-order differential equations. The results are that considerable effort must be expended to obtain the eigenvalues (resonances) and eigenvectors (mode shapes) of the equations of motion.

We will show that the formulation of the equations of motion using derivatives of fractional order also produces higher order matrix equations to solve. However, our fractional derivative model of the frequency-dependent mechanical properties typically requires only five empirical parameters. This is fewer parameters than are usually required with the corresponding standard linear viscoelastic model. We believe that relatively few empirical parameters are required in the fractional derivative models because they are consistent with the physical principles involved. Consequently, we feel that fractional derivative models are attractive as a tool of engineering analysis.

The Fractional Derivative Viscoelastic Model

Early observations of the mechanical properties of viscoelastic materials by Nutting indicated that the stress relaxation phenomenon appeared to be proportional to time raised to fractional powers.³ Later observations by Gemant showed that the frequency dependence of the mechanical properties varies as frequency raised to fractional powers, and he suggested that differentials of fractional order be used to model materials.^{4,5} More recently, Scott-Blair proposed that fractional derivatives could be used to relate time-dependent stress and strain in viscoelastic materials.⁶ Scott-Blair's use of fractional calculus simultaneously modeled the observations of Nutting and Gemant. Fifteen years ago, Caputo independently echoed Scott-Blair's observations on the use of fractional calculus. Caputo used fractional derivatives to model the behavior of viscoelastic geological strata.^{7,8} In addition, Caputo and Minardi concluded from experimental observations that fractional derivative relationships were valid for some metals and glasses.⁹

The fractional derivative model put forward here is a generalization of both Caputo's and Scott-Blair's models. This modified model is based on the observed mechanical behavior of 30 materials (elastomers and glassy enamels).¹⁰ It is important to note that fractional derivative relationships, derived from first principles,¹¹ for uncrosslinked polymer solids are almost identical in form to Scott-Blair's model and to the model presented here.

The general form of our fractional derivative viscoelastic model is

$$\sigma(t) + \sum_{m=1}^M b_m D^{\beta_m} \langle \sigma(t) \rangle = E_0 \epsilon(t) + \sum_{n=1}^N E_n D^{\alpha_n} \langle \epsilon(t) \rangle \quad (2)$$

where the time-dependent stress fields are related to time-dependent strain fields through series of derivatives of fractional order. Experimental observations indicate that many viscoelastic materials can be modeled by retaining only the first fractional derivative term in each series in Eq. (2). The result is a viscoelastic model with five parameters, b , E_0 , E_1 , α , and β .

$$\sigma(t) + b D^{\beta} \langle \sigma(t) \rangle = E_0 \epsilon(t) + E_1 D^{\alpha} \langle \epsilon(t) \rangle \quad (3)$$

The fractional derivatives are defined by

$$D^{\alpha} \langle x(t) \rangle = \frac{1}{\Gamma(1-\alpha)} \frac{d}{dt} \int_0^t \frac{x(\tau)}{(t-\tau)^{\alpha}} d\tau \quad 0 < \alpha < 1 \quad (4)$$

This fractional derivative operator has the property in the Laplace transform domain

$$L \langle D^{\alpha} \langle x(t) \rangle \rangle = s^{\alpha} L \langle x(t) \rangle \quad (5)$$

that the transform of the fractional derivative of $x(t)$ is equal to s^{α} times the transform of $x(t)$. This property can be demonstrated by taking the Laplace transform of Eq. (4),

$$L \langle x(t) \rangle = \int_0^{\infty} x(t) e^{-st} dt \quad (6)$$

A similar relationship exists in the Fourier transform domain. By taking the Fourier transform,

$$F \langle x(t) \rangle = \int_{-\infty}^{\infty} x(t) e^{-i\omega t} dt \quad (7)$$

of Eq. (4), a relationship similar to Eq. (5) results.

$$F \langle D^{\alpha} \langle x(t) \rangle \rangle = (i\omega)^{\alpha} F \langle x(t) \rangle \quad (8)$$

The Fourier transform of the fractional derivative of order α of $x(t)$ is $(i\omega)^{\alpha}$ times the Fourier transform of $x(t)$. Taking the Fourier transform of the five parameter viscoelastic model, Eq. (3), yields

$$\sigma^*(i\omega) + b(i\omega)^{\beta} \sigma^*(i\omega) = E_0 \epsilon^*(i\omega) + E_1 (i\omega)^{\alpha} \epsilon^*(i\omega) \quad (9)$$

where $\sigma^*(i\omega)$ and $\epsilon^*(i\omega)$ are the transform of the stress and strain histories, respectively. Factoring and dividing terms in this operation produces

$$\sigma^*(i\omega) = \frac{E_0 + E_1 (i\omega)^{\alpha}}{1 + b(i\omega)^{\beta}} \epsilon^*(i\omega) \quad (10)$$

The model suggests that the frequency dependent modulus is a function of fractional powers of frequency. This is consistent with the observation of Gemant alluded to earlier.

The five parameters are determined by a least squares fit of this model to the frequency-dependent mechanical properties of the material. Such fits have been obtained for several materials. Figure 1 demonstrates the excellent agreement between the model and the mechanical properties at 550°C of a Corning glass doped with oxides of aluminum, sodium, and cobalt (7.5% Al_2O_3 , 3% Na_2O , 1% Co_2O_3). The parameters of the model are

$$E_0 = 4.15 \times 10^9 \text{ N/m}^2 \quad (11)$$

$$E_1 = 1.09 \times 10^{11} \text{ N} \cdot (\text{s})^{0.641} / \text{m}^2 \quad (12)$$

$$b = 3.50 (\text{s})^{0.631} \quad (13)$$

$$\alpha = 0.641 \quad (14)$$

$$\beta = 0.631 \quad (15)$$

These results are typical. The five parameters consistently describe two high-order curves simultaneously. In many cases, taking $\alpha = \beta$ produces a very satisfactory fit. Data given

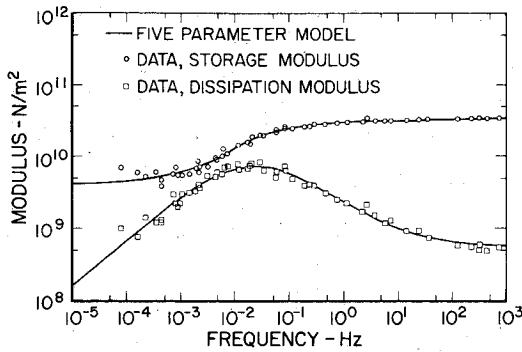


Fig. 1 Mechanical properties of Corning 10.

in Fig. 1 were obtained¹² for a range of temperatures and frequencies and reduced to a single temperature through the reduced frequency procedure.¹³ These data and curves describe the same material at 610°C if the frequency is multiplied by 10^2 , at 690°C if the frequency is multiplied by 10^4 , and at 840°C if the frequency is multiplied by 10^6 .

The following section is an outline of the construction and solution of the finite element equations of motion for viscoelastically damped structures when Eq. (3) is used to model the damping material. The Laplace transform is used in this development. Before proceeding it is useful to present the relationship between the transform of stress $\sigma^*(s)$ and strain $\epsilon^*(s)$ for the five parameter model,

$$\sigma^*(s) = \frac{E_0 + E_1 s^\alpha}{1 + b s^\beta} \epsilon^*(s) \quad (16)$$

or

$$\sigma^*(s) = \mu^*(s) \epsilon^*(s) \quad (17)$$

where

$$\mu^*(s) = \frac{E_0 + E_1 s^\alpha}{1 + b s^\beta} \quad (18)$$

This modulus is used to construct the stiffness matrices of the viscoelastic elements in the damped structure.

To this point, only a one-dimensional or uniaxial stress-strain relationship has been described. However, the fractional calculus does not suffer from such a limitation. The presentation of a complete three-dimensional relationship is given in Ref. 1. Also presented in Ref. 1 is a complete derivation of the finite element equations of motion for structures damped with multiple viscoelastic materials. What follows here is an outline of this derivation. It is assumed, for the sake of simplicity in notation, that a single viscoelastic material undergoing uniform, uniaxial stress (strain) is used to damp the structure.

The Construction and Solution of the Equations of Motion

Having made several observations about fractional derivative material models, it is appropriate to present the method used in the analysis of viscoelastically damped structures. Because of its popularity and the flexibility it affords in the analyses of structures of engineering interest, the following discussion is presented in terms of a finite element formulation. Use of the fractional calculus model is, of course, not limited to finite element applications.

The cornerstone of any finite element approach is the construction of the stiffness matrices for each of the finite elements in the structure. Normally, the stiffness matrix for each elastic finite element is constructed by using assumed displacement methods or assumed stress methods. The

formulation of the stiffness matrices for the finite element in the viscoelastic regions of the structure, however, must be limited to those methods that do not constrain the stresses in each finite element to be in equilibrium with the forces at the nodes of the element. This restriction is generated by the requirement that viscoelastic stresses be dependent on strain-time histories. Finite element methods constraining stresses within an element to be in equilibrium with the nodal forces, e.g., assumed stress methods, are not consistent with the assumption that stresses be dependent on the local strain history.¹⁴ Consequently, assumed displacement methods for constructing viscoelastic finite element stiffness matrices are used in formulating the equations of motion.

The stiffness matrix of a viscoelastic finite element is constructed using the elastic-viscoelastic correspondence principle.¹⁵ The stiffness matrix is first formulated as though the material were elastic. The element stiffness matrix is then separated into two matrices, one containing those terms proportional to the Lamé constant λ and the other containing those terms proportional to the Lamé constant μ ,

$$[K_e] = \lambda [K'_e] + \mu [K''_e] \quad (19)$$

At this point the transforms of the viscoelastic moduli, $\mu^*(s)$ and $\lambda^*(s)$, are substituted in place of the Lamé constants. Since this development is limited to the consideration of uniform, uniaxial shear strain, the viscoelastic stiffness matrix takes the form

$$[K_e] = \mu^*(s) [K''_e] \quad (20)$$

Substituting the five parameter model for $\mu^*(s)$ [Eq. (18)] into Eq. (20) produces

$$[K_e] = \frac{E_0 + E_1 s^\alpha}{1 + b s^\beta} [K''_e] \quad (21)$$

At this point the stiffness matrices for both the elastic and viscoelastic finite elements in the structure are used to construct the stiffness matrix of the total structure in the traditional manner. The resulting stiffness matrix differs from conventional stiffness matrices in that some matrix elements are functions of the Laplace parameter s . The resulting equations of motion for the total structure in the transform domain are

$$s^2 [M] \{X(s)\} + [K(s)] \{X(s)\} = \{F(s)\} \quad (22)$$

Since the stiffness matrix contains functions of the Laplace parameter, it is clear that conventional techniques for decoupling the equations of motion do not apply. Consequently, a different approach for decoupling the equations of motion is adopted.

The method used is similar to the method developed by Foss¹⁶ for decoupling the equations of motion having non-proportional viscous damping, i.e., a damping matrix not a linear combination of the mass and stiffness matrices. Those equations are

$$[M] \{\ddot{x}(t)\} + [C] \{\dot{x}(t)\} + [K] \{x(t)\} = \{f(t)\} \quad (23)$$

These equations of motion are posed in the form

$$\frac{d}{dt} \left\{ \begin{bmatrix} 0 & M \\ M & C \end{bmatrix} \begin{Bmatrix} \dot{x} \\ x \end{Bmatrix} \right\} + \begin{bmatrix} -M & 0 \\ 0 & K \end{bmatrix} \begin{Bmatrix} \dot{x} \\ x \end{Bmatrix} = \begin{Bmatrix} 0 \\ f(t) \end{Bmatrix} \quad (24)$$

where the top set of partitioned matrix equations is satisfied identically and the lower set of matrix equations is the original equations of motion [Eq. (23)]. The efficacy of this approach

is that an orthogonal transformation can be found that diagonalizes the two real, square, symmetric matrices in Eq. (24), while obtaining an orthogonal transformation for the original equations [Eq. (23)] is usually not possible.

To put the equations of motion of our viscoelastically damped structure into a form similar to Eq. (24), we multiply the equations of motion by the denominator of $\mu^*(s)$, which is $(1 + bs^\beta)$. Next we segregate matrix elements of the equation of motion into matrices having common powers of the Laplace parameter. The resulting form of the equations of motion is

$$[s^{2+\beta}b[M] + s^2[M] + s^\alpha E_I[K_I] + s^\beta b[K_2] + [K_3]]\{X(s)\} = (I + bs^\beta)\{F(s)\} \quad (25)$$

where the terms involving $[K_I]$ through $[K_3]$ are the stiffness matrix in Eq. (22) multiplied by $(1 + bs^\beta)$.

The next step is to identify the smallest common denominator of the fractions α and β , referred to as m . Having obtained m , the left side of Eq. (25) is expressed as a matrix sum and the equations of motion take the form

$$\sum_{j=0}^J [A_j] \{s^{j/m} X(s)\} = (I + bs^\beta)\{F(s)\} \quad (26)$$

Clearly, some of the matrices $[A_j]$ will be zero, and the nonzero $[A_j]$ come from $[M]$ and $[K_I]$ through $[K_3]$ in Eq. (25). Note that $J = m(2 + \beta)$.

The problem now is how to pose the equations of motion in terms of two real, square, symmetric matrices for which we can obtain an orthogonal transformation and decouple the equations of motion. The answer is to cast the equations of motion in the following format:

$$s^{1/m}[\tilde{M}]\{\tilde{X}(s)\} + [\tilde{K}]\{\tilde{X}(s)\} = \{\tilde{F}(s)\} \quad (27)$$

$$[\tilde{M}] = \begin{bmatrix} [0] & [0] & \cdots & [0] & [A_J] \\ [0] & [0] & \cdots & [A_J] & [A_{J-1}] \\ \vdots & \vdots & \ddots & \vdots & \vdots \\ [0] & [A_J] & \cdots & [A_3] & [A_2] \\ [A_J] & [A_{J-1}] & \cdots & [A_2] & [A_1] \end{bmatrix} \quad (28)$$

$$[\tilde{K}] = \begin{bmatrix} [0] & [0] & \cdots & [0] & [-A_J] & [0] \\ [0] & [0] & \cdots & [-A_J] & [-A_{J-1}] & [0] \\ [0] & [0] & \cdots & [-A_{J-1}] & [-A_{J-2}] & [0] \\ \vdots & \vdots & \ddots & \vdots & \vdots & \vdots \\ [-A_J] & [-A_{J-1}] & \cdots & [-A_3] & [-A_2] & [0] \\ [0] & [0] & \cdots & [0] & [0] & [A_0] \end{bmatrix} \quad (29)$$

$$\{\tilde{X}(s)\} = \begin{bmatrix} s^{(J-1)/m} \{X(s)\} \\ s^{(J-2)/m} \{X(s)\} \\ \vdots \\ s^{1/m} \{X(s)\} \\ I \{X(s)\} \end{bmatrix} \quad (30)$$

$$\{\tilde{F}(s)\} = \begin{bmatrix} \{0\} \\ \{0\} \\ \vdots \\ \{0\} \\ (I + bs^\beta)\{F(s)\} \end{bmatrix} \quad (31)$$

Notice that the two large matrices are real, square, and symmetric because the submatrices $[A_j]$ are themselves real, square, and symmetric. Also note that the lowest set of partitioned matrix equations are the equations of motion for the structure [Eq. (26)] and all of the upper sets of matrix equations are satisfied identically.

This expanded form of the equations of motion differs from Eq. (24) in that the equations are posed in the transform domain, but the fractional powers of s in the submatrices of the column matrices correspond to derivatives of fractional order. Equation (27) may be returned to the time domain, or Eq. (24) brought to the transform domain. The major difference, then, between Eq. (27), the expanded equations of motion, and Eq. (24) is that the latter are posed in terms of derivatives of integer order.

It is clear that the order of the expanded equations for structures of engineering interest could be very large and the size of the matrices prohibitive to manipulate even on the electronic computer. However, this does not diminish the value of the expanded equations of motion for the orthogonal transformation decoupling the expanded equations of motion can be constructed and the decoupling procedure accomplished without directly using the expanded equations of motion.¹

The orthogonal transformation for the expanded equation is constructed using homogeneous solutions for the original equations of motion [Eq. (25)]. These solutions satisfy the equation

$$\begin{aligned} &[\tilde{\lambda}_n^{(2+\beta)m} b[M] + \tilde{\lambda}_n^{2m}[M] + \tilde{\lambda}_n^{\alpha m} E_I[K_I] \\ &+ \tilde{\lambda}_n^{\beta m} b[K_2] + [K_3]]\{\phi_n\} = 0 \end{aligned} \quad (32)$$

which is the homogeneous form of Eq. (25). The eigenvalues $\tilde{\lambda}_n$ and the eigenvectors $\{\phi_n\}$ for this equation can be found using matrix iteration techniques similar to those commonly used for finding mode shapes and resonant frequencies for undamped structures.¹

Given that the expanded equations of motion can be decoupled using constructions based on homogeneous solutions to Eq. (25), it is appropriate to present the general form of the solution to the expanded equations of motion,¹

$$\{X(s)\} = \sum_{n=1}^N \frac{\{\phi_n\}^T \{F(s)\} (I + bs^\beta)}{m_n (s^{1/m} - \tilde{\lambda}_n)} \{\phi_n\} \quad (33)$$

This solution is the transform of the structural displacement time histories $\{X(s)\}$ in terms of the transforms of the applied loads $\{F(s)\}$. $\{\phi_n\}$ and $\tilde{\lambda}_n$ are the solutions to Eq. (32), $(1 + bs^\beta)$ is the dominator of $\mu^*(s)$, and N is the order of the matrices $[\tilde{M}]$ and $[\tilde{K}]$ in the expanded equations of motion. m_n is a modal constant, similar in form to a modal mass, and is defined as

$$\{\tilde{\phi}_n\}^T [\tilde{M}] \{\tilde{\phi}_n\} = m_n \quad (34)$$

where $\{\tilde{\phi}_n\}$ is the n th eigenvector of the expanded equations of motion. $\{\tilde{\phi}_n\}$ is constructed from $\tilde{\lambda}_n$ and $\{\phi_n\}$, the solutions to Eq. (32).

Having presented the transform of the structural response, the next issue to be confronted is the existence of the inverse

transform of the structural response, namely the existence of the time history of the motion of the modes of the finite element model. We are particularly interested in the structural response for impulsive loading, i.e., when the applied forces are equal to the Dirac delta function. Observing that the transform of the delta function is one, the transform of the impulse response is

$$\{\hat{X}(s)\} = \sum_{n=1}^N \frac{\{\phi_n\}^T \{I\} (I + bs^\beta)}{m_n (s^{1/m} - \lambda_n)} \{\phi_n\} \quad (35)$$

The inverse transform of $\{\hat{X}(s)\}$, $\{\hat{x}(t)\}$, exists and is real, continuous, and causal when 1) $\{\hat{X}(s)\}$ is analytic for $\text{Re}(s) > 0$, 2) $\{\hat{X}(s)\}$ is real for s real and positive, and 3) $\{\hat{X}(s)\}$ is order $s^{-\gamma}$, where $\gamma > 1$, for $|s|$ large in the right half s plane. The proof that these three conditions are met is straightforward.¹

Consequently, the time-dependent response of the structure to impulse loading exists and is real, continuous, and causal. Using contour integration and the residue theorem to determine the form of the impulse response produces

$$\{\hat{x}(t)\} = \frac{1}{\pi} \text{Im} \left\langle \int_0^\infty \{\hat{X}(re^{-i\pi})\} e^{-rt} dr \right\rangle + \sum_j \frac{m\lambda_j^{m-1} \{\phi_j\}^T \{I\} (I + b\lambda_j^{\beta m})}{m_j} \{\phi_j\} e^{\lambda_j t} \quad (36)$$

The essential details of the process used in passing from Eq. (35) to Eq. (36) are given in the Appendix.

Note that the response of the structure has two parts, one part being a sum of decaying sinusoids and the other an integral that decreases with increasing time. The integral does not decrease exponentially. In fact, the integral is asymptotic to $t^{-\eta}$ for large t , where η is greater than one. Therefore, the integral dominates the response for a time long after the loading. This component of the response describes the nonoscillatory return of the structure to its unloaded equilibrium position. It is also a manifestation of the power law stress relaxation phenomena observed by Nutting.³

Example

Since the method introduces unfamiliar notations and procedures, an example of its application is helpful. We will demonstrate the process followed in analyzing systems described by fractional derivatives through the example depicted in Fig. 2. The tension member is fixed at both ends, but supported at two interior points by shear dampers, consisting of pads of a material described by the five-parameter fractional derivative model. Only longitudinal motion resulting from forces applied at the nodal points is considered.

The finite element representation of this system, after transforming to the Laplace domain, is

$$s^2 [M] \{X\} + [D(s)] \{X\} + [K] \{X\} = \{F\} \quad (37)$$

The mass and stiffness matrices are developed from rod elements, and the damping matrix is developed from the nodal force relationship that results when the shear pads are

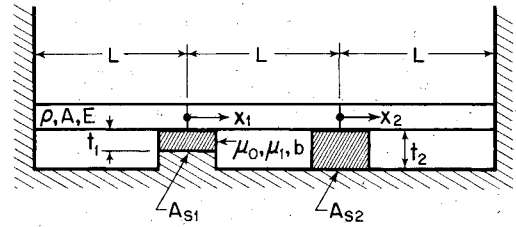


Fig. 2 Elastic rod supported by elastomeric pads.

described by the five parameter model, i.e.,

$$\begin{aligned} & \left\{ \{F_n\} + b \frac{d^\beta}{dt^\beta} \langle \{F_n\} \rangle \right\} \\ & = \begin{bmatrix} A_{s1}/t_1 & 0 \\ 0 & A_{s2}/t_2 \end{bmatrix} \left\{ \mu_0 \{X\} + \mu_1 \frac{d^\alpha}{dt^\alpha} \langle \{X\} \rangle \right\} \end{aligned} \quad (38)$$

The resulting numerical work is simplified by the introduction of a dimensionless scaled time τ defined through

$$t = c\tau \quad (39)$$

For this example, s will be taken as the dimensionless Laplace transform parameter corresponding to the dimensionless time. The scale factor may be incorporated into the damping and mass matrices to yield

$$M = \frac{\rho AL}{6c^2} \begin{bmatrix} 4 & 1 \\ 1 & 4 \end{bmatrix} \quad (40)$$

$$K = \frac{AE}{L} \begin{bmatrix} 2 & -1 \\ -1 & 2 \end{bmatrix} \quad (41)$$

$$D = \frac{\mu_0 + \mu_1 (s/c)^{1/2}}{1 + b(s/c)^{1/2}} \begin{bmatrix} A_{s1}/t_1 & 0 \\ 0 & A_{s2}/t_2 \end{bmatrix} \quad (42)$$

Damper properties are described by μ_0 , μ_1 , and b . For convenience, both fractional derivatives have been taken to be $1/2$. Each shear pad is of contact area A_s , but the thicknesses t_1 and t_2 are different to insure that the damping matrix is nonproportional. All rods are of length L , density ρ , and cross-sectional area A .

Introducing the following numerical values:

$$\begin{aligned} A &= 10^{-3} \text{ m}^2 & A_{s1} &= A_{s2} = 10^{-3} \text{ m}^2 \\ t_1 &= 2 \times 10^{-3} \text{ m} & t_2 &= 40 \times 10^{-3} \text{ m} \\ \rho &= 1.25 \times 10^4 \text{ kg/m}^3 & E &= 200 \times 10^9 \text{ N/m}^2 \\ \mu_0 &= 4 \times 10^7 \text{ N/m}^2 & \mu_1 &= 4\sqrt{5} \times 10^5 \text{ N} \cdot \text{s}^{1/2} / \text{m}^2 \\ b &= \sqrt{5} \times 10^{-3} \text{ s}^{1/2} & L &= 1 \text{ m} \end{aligned}$$

and a convenient scale factor, $c = 5 \times 10^{-4} \text{ s}$ leads to the following system, see Eq. (22)

$$\begin{aligned} & s^2 \begin{bmatrix} 0.33 & 0.0825 \\ 0.0825 & 0.33 \end{bmatrix} \begin{Bmatrix} X_1(s) \\ X_2(s) \end{Bmatrix} + \begin{bmatrix} 4.0 + (0.2 + 0.2s^{1/2})(1.0 + 0.1s^{1/2})^{-1} & -2 \\ -2 & 4.0 + (0.01s^{1/2})(1.0 + 0.1s^{1/2})^{-1} \end{bmatrix} \\ & \times \begin{Bmatrix} X_1(s) \\ X_2(s) \end{Bmatrix} = \begin{Bmatrix} F_1(s) \\ F_2(s) \end{Bmatrix} \times 10^{-8} \text{ m/N} \end{aligned} \quad (43)$$

Clearing the Laplace parameter from the denominator of the damping matrix produces equations in the form of Eq. (25),

$$\begin{aligned} & \left[s^{5/2}(0.1) \begin{bmatrix} 0.33 & 0.0825 \\ 0.0825 & 0.33 \end{bmatrix} + s^2 \begin{bmatrix} 0.33 & 0.0825 \\ 0.0825 & 0.33 \end{bmatrix} \right. \\ & + s^{1/2}(0.01) \begin{bmatrix} 2.0 & 0.0 \\ 0.0 & 1.0 \end{bmatrix} + s^{1/2}(0.1) \begin{bmatrix} 4.0 & -2.0 \\ -2.0 & 4.0 \end{bmatrix} \\ & \left. + \begin{bmatrix} 4.2 & -2.0 \\ -2.0 & 4.01 \end{bmatrix} \right] \begin{Bmatrix} X_1(s) \\ X_2(s) \end{Bmatrix} = \begin{Bmatrix} \bar{F}_1(s) \\ \bar{F}_2(s) \end{Bmatrix} \quad (44) \end{aligned}$$

The load vector F has been manipulated into a new load vector \bar{F} through this process.

The homogeneous equations of motion produce a characteristic value problem

$$\begin{aligned} & \tilde{\lambda}^5 \begin{bmatrix} 0.03300 & 0.00825 \\ 0.00825 & 0.03300 \end{bmatrix} + \tilde{\lambda}^4 \begin{bmatrix} 0.3300 & 0.0825 \\ 0.0825 & 0.3300 \end{bmatrix} \\ & + \tilde{\lambda} \begin{bmatrix} 0.60 & -0.20 \\ -0.20 & 0.41 \end{bmatrix} + \begin{bmatrix} 4.2 & -2.0 \\ -2.0 & 4.01 \end{bmatrix} \{\phi\} = \{0\} \quad (45) \end{aligned}$$

where $\tilde{\lambda}$ corresponds to square roots of the Laplace parameter s . This fifth-order eigenvalue problem for a two degree-of-freedom system will lead to 10 (complex) eigenvalues $\tilde{\lambda}$ and 10 (complex) eigenvectors $\{\phi\}$.

We now solve the homogeneous system of the expanded equations of motion (26) and (27). For this example,

$$[A_0] = \begin{bmatrix} 4.2 & -2.0 \\ -2.0 & 4.01 \end{bmatrix} \quad (46)$$

$$[A_1] = \begin{bmatrix} 0.60 & -0.20 \\ -0.20 & 0.41 \end{bmatrix} \quad (47)$$

$$[A_2] = \begin{bmatrix} 0.0 & 0.0 \\ 0.0 & 0.0 \end{bmatrix} = [A_3] \quad (48)$$

$$[A_4] = \begin{bmatrix} 0.3300 & 0.0835 \\ 0.0825 & 0.3300 \end{bmatrix} \quad (49)$$

$$[A_5] = \begin{bmatrix} 0.03300 & 0.00825 \\ 0.00825 & 0.03300 \end{bmatrix} \quad (50)$$

The expanded equations of motion are of order 10, leading to 10 complex eigenvalues and the complex eigenvectors. The eigenvalues and eigenvectors were found using a modified form of matrix iteration,¹ with results as shown in Table 1. As expected, the complex eigenvalues and eigenvectors occur in complex conjugate pairs. One can now return to Eq. (33) and construct the transform of the response of the structure for a general loading. The computation of the inverse for the case of an impulse loading is demonstrated in the Appendix.

The solutions to the homogeneous problem contain much important information concerning the response of the system.

Table 1 Eigenvalues and eigenvectors for the example problem

$\tilde{\lambda}_1 = 1.071768 + i1.099794$	$\{\phi_1\} = \begin{Bmatrix} 1.000 + i0.0000 \\ 1.040 + i0.0165 \end{Bmatrix}$
$\tilde{\lambda}_2 = 1.071768 - i1.099794$	$\{\phi_2\} = \begin{Bmatrix} 1.000 + i0.0000 \\ 1.040 - i0.0165 \end{Bmatrix}$
$\tilde{\lambda}_3 = -1.073498 + i1.028611$	$\{\phi_3\} = \begin{Bmatrix} 1.000 + i0.0000 \\ 1.001 + i0.0238 \end{Bmatrix}$
$\tilde{\lambda}_4 = -1.073498 - i1.028611$	$\{\phi_4\} = \begin{Bmatrix} 1.000 + i0.0000 \\ 1.001 - i0.0238 \end{Bmatrix}$
$\tilde{\lambda}_5 = 1.581998 + i1.601989$	$\{\phi_5\} = \begin{Bmatrix} 1.000 + i0.0000 \\ -0.9713 + i0.0120 \end{Bmatrix}$
$\tilde{\lambda}_6 = 1.581998 - i1.601989$	$\{\phi_6\} = \begin{Bmatrix} 1.000 + i0.0000 \\ -0.9713 - i0.0120 \end{Bmatrix}$
$\tilde{\lambda}_7 = -1.584631 + i1.547150$	$\{\phi_7\} = \begin{Bmatrix} 1.000 + i0.0000 \\ -1.002 + i0.0240 \end{Bmatrix}$
$\tilde{\lambda}_8 = -1.584631 - i1.547150$	$\{\phi_8\} = \begin{Bmatrix} 1.000 + i0.0000 \\ -1.002 - i0.0240 \end{Bmatrix}$
$\tilde{\lambda}_9 = -9.997418 + i0.0$	$\{\phi_9\} = \begin{Bmatrix} 1.000 + i0.0 \\ 4.462 + i0.0 \end{Bmatrix}$
$\tilde{\lambda}_{10} = -9.99385 + i0.0$	$\{\phi_{10}\} = \begin{Bmatrix} 1.000 + i0.0 \\ -0.448 + i0.0 \end{Bmatrix}$

Since the solutions are not in a familiar form, however, the expected response characteristics may not be recognized in the numerical results. It is useful to look in the results for what one would expect to see in the response of a two degree-of-freedom system. First, we expect to see two eigenvalues and two eigenvectors corresponding to two normal modes. The two eigenvalues should correspond to two natural frequencies. If the dampers were not present, the second frequency should be twice the value of the first. The mode shape corresponding to the first frequency should indicate in-phase motion of the nodes and the mode shape for the second frequency should indicate out-of-phase motion. In addition, one would expect the response of the system to be described by real functions of time. With these anticipated characteristics of the physical response in mind, let us return to the numerical results.

The eigenvalues $\tilde{\lambda}$ were introduced as square roots of the dimensionless Laplace parameter s . It follows that non-dimensional eigenvalues correspond to square roots of dimensionless complex natural frequencies. Squaring the first, second, fifth, and sixth eigenvalues in Table 1 produces two conjugate pairs, where each conjugate pair corresponds to a natural frequency of the system. We find $\omega_1 = \tilde{\lambda}_1^2 = -0.0609 + i2.357$, $\omega_2 = \tilde{\lambda}_2^2 = -0.0637 + i5.069$. It should be noted that each of these frequencies has been computed with the frequency-dependent material properties appropriate to that frequency. The dimensionless frequencies are readily converted into radians/second by dividing by the scale factor c . The frequencies are 750 and 1614 cps. For the hypothetical elastomer used in this example, the magnitude of the modulus increases 52% over that range. The magnitude of one frequency is approximately twice the magnitude of the other, as expected. Since the real parts are small, the system is lightly damped. The remaining eigenvalues do not denote further resonances, but describe the nonoscillatory behavior of the damped structure. These eigenvalues are recognized by the fact that the phase angle of their squares do not lie in the range $-180 < \theta \leq 180$. Thus, the natural frequencies are predicted and identified.

The eigenvectors associated with the eigenvalues identifying resonant behavior, (the first, second, fifth, and sixth) also occur in conjugate pairs. The first and second eigenvectors combine to produce the first mode shape and indicate real, in-phase motion of the nodes. Similarly, the fifth and sixth eigenvectors combine to produce the second mode shape and indicates real, out-of-phase motion. The remaining six eigenvectors combine with the conjugate temporal terms to show that the nonoscillatory portion of the motion of the structure is also real.

Conclusion

We conclude that the equations of motion for viscoelastically damped structures can be constructed and solved in a reasonably straightforward manner when the mechanical behavior of the viscoelastic material is portrayed by the fractional calculus model. The attractiveness of these models is that they are consistent with the physical principles and that they accurately describe the mechanical properties of a variety of materials over wide ranges of frequency. The small number of empirical parameters needed with these models facilitates the process of obtaining a least squares fit to the mechanical properties of the materials and reduces the effort required to solve the resulting equations of motion.

The fractional calculus approach is an encompassing method for the analysis of damped structures. The approach begins with the molecular theory of polymer solids, proceeds to generate accurate mathematical models for viscoelastic behavior, results in well-posed equations of motion, and concludes with closed-form solutions for structures of engineering interest.

Appendix: Calculation of the Response of Impulsive Loading

The final step in determining the impulse response of the structure is to calculate the inverse transform of the Laplace transform of the response to impulsive loading,

$$\{\hat{x}(t)\} = L^{-1}\{\{\hat{X}(s)\}\}$$

$$= L^{-1}\left\langle \sum_{n=1}^N \frac{\{\phi_n\}^T \{I\} (I + b s^\beta)}{m_n (s^{1/m} - \lambda_n)} \{\phi_n\} \right\rangle \quad (A1)$$

The inverse transform integral

$$L^{-1}\{\{\hat{X}(s)\}\} = \frac{1}{2\pi i} \int_{\gamma-i\infty}^{\gamma+i\infty} e^{st} \{\hat{X}(s)\} ds \quad (A2)$$

is evaluated using the residue theorem from the calculus of a complex variable.

The closed contour of integration, used in conjunction with the residue theorem, is given in Fig. A1. The contour is divided into six segments and the direction of integration along each segment is indicated by the arrows. Segments 3-5 of the contour are required, because the branch cut and branch point of the function $s^{1/m}$ are taken to be along the negative real axis and at the origin of the s plane, respectively.

The residue theorem states that the integral along the closed contour, divided by $2\pi i$, is equal to the sum of the residues of the poles of the integrand. In this case, the statement of the residue theorem translates into

$$\frac{1}{2\pi i} \int_I \{\hat{X}(s)\} e^{st} ds = -\frac{1}{2\pi i} \sum_{k=2}^6 \int_k \{\hat{X}(s)\} e^{st} ds + \sum_j \{b_j\} \quad (A3)$$

where the index indicates the contour over which the integration is to be performed, and $\{b_j\}$ are the residues of the poles of $\{X(s)\}$ enclosed by the contour.

The integrals on the segments of the closed contour are evaluated for the case where the length of segment 1 is extended indefinitely in the positive and negative imaginary directions,

$$\int_I \{\hat{X}(s)\} e^{st} ds = \int_{\gamma-i\infty}^{\gamma+i\infty} \{\hat{X}(s)\} e^{st} ds \quad (A4)$$

and, as a result, Eq. (A2) becomes

$$\begin{aligned} \frac{1}{2\pi i} \int_{\gamma-i\infty}^{\gamma+i\infty} \{\hat{X}(s)\} e^{st} ds \\ = -\frac{1}{2\pi i} \sum_{k=2}^6 \int_k \{\hat{X}(s)\} e^{st} ds + \sum_j \{b_j\} \end{aligned} \quad (A5)$$

showing that one need evaluate the right side of Eq. (A5) to obtain the inverse transform.

To maintain the continuity of the closed contour, the radii of segments 2 and 6 are increased indefinitely and segments 3 and 5 are extended indefinitely in the negative real direction. When the radii of contours 2 and 6 are increased indefinitely, it can be demonstrated that the resulting value of the integrals along these two segments is zero. Similarly, it can be shown that the integral along contour 4 goes to zero as the radius of the contour is decreased indefinitely. The integrals along contours 3 and 5 are not zero, nor do they add to zero. Rather,

$$\begin{aligned} \int_3 e^{st} \{\hat{X}(s)\} ds + \int_5 e^{st} \{\hat{X}(s)\} ds \\ = \frac{1}{\pi} \text{Im} \left\langle \int_0^\infty \{\hat{X}(e^{-i\pi})\} e^{-rt} dr \right\rangle \end{aligned} \quad (A6)$$

The residues $\{b_j\}$ are evaluated by using conventional techniques

$$\{b_j\} = \lim_{s \rightarrow \lambda_j^m} (s - \lambda_j^m) \{\hat{X}(s)\} e^{st} \quad (A7)$$

For the impulsive load, the result is

$$\{b_j\} = \frac{m \lambda_j^{m-1} \{\phi_j\}^T \{I\} (I + b \lambda_j^{\beta m})}{m_j} \{\phi_j\} e^{\lambda_j^m t} \quad (A8)$$

Since the integrals on contours 2, 4, and 6 are zero, Eqs. (A6) and (A8) enable the evaluation of Eq. (A5),

$$\begin{aligned} \{\hat{x}(t)\} &= \frac{1}{\pi} \text{Im} \left\langle \int_0^\infty \{\hat{X}(re^{-i\pi})\} e^{-rt} dr \right\rangle \\ &+ \sum_j \frac{m \lambda_j^{m-1} \{\phi_j\}^T \{I\} (I + b \lambda_j^{\beta m})}{m_j} \{\phi_j\} e^{\lambda_j^m t} \end{aligned} \quad (A9)$$

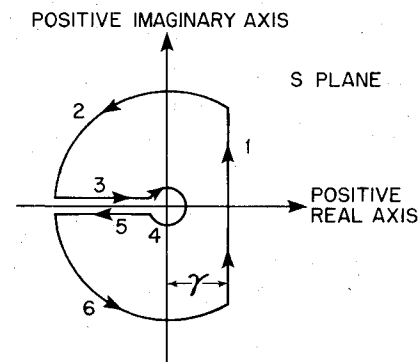


Fig. A1 Integration contour for inversion transform.

Thus, we have obtained the impulse response of the system.

The summation over the index j in the impulse response [Eq. (A9)] differs from the sum over the index n in Eq. (A1). The poles of the Laplace transform shown in Eq. (A1) $\tilde{\lambda}_n$ are originally found in the $s^{1/m}$ plane. Since the inverse Laplace transform is evaluated in the s plane, the transformation $\tilde{\lambda}^m$ must be applied to bring the poles into the s plane. Under the transformation $\tilde{\lambda}^m$ many of the poles in the λ plane map onto Riemann surfaces not included within the contour of integration in the s plane. The residues of these poles do not contribute to the response of the system. The index j in the summation is therefore allowed to assume only those values corresponding to poles within the closed contour in the s plane.

Acknowledgments

This work was sponsored by the Metals Behavior Branch, Metals and Ceramics Division of the Materials Laboratory, Wright Aeronautical Laboratories, Wright-Patterson AFB, Ohio. In particular, we are indebted to Drs. Jack Henderson, David Jones, and Ted Nicholas of the Metals Behavior Branch for their encouragement and suggestions. Parts of this paper are extracted from a Ph.D. dissertation submitted by the first author to the Air Force Institute of Technology.

References

- ¹Bagley, R. L., "Applications of Generalized Derivatives to Viscoelasticity," Air Force Materials Laboratory, TR-79-4103, Nov. 1979.
- ²Crandall, S. H., "Dynamic Responses of Systems with Structural Damping," *Air, Space and Instruments, Draper Anniversary Volume*, edited by H. S. Lee, McGraw-Hill Book Co., New York, 1963, pp. 183-193.
- ³Nutting, P. G., "A New General Law of Deformation," *Journal of the Franklin Institute*, Vol. 191, May 1921, pp. 679-685.
- ⁴Gemant, A., "A Method of Analyzing Experimental Results Obtained from Elasto-Viscous Bodies," *Physics*, Vol. 7, 1936, pp. 311-317.
- ⁵Gemant, A., "On Fractional Differentials," *Philosophical Magazine*, Vol. 25, 1938, pp. 540-549.
- ⁶Graham, A., "The Phenomenological Method in Rheology," *Research*, London, 1953, pp. 92-96.
- ⁷Caputo, M., *Elasticità e Dissipazione*, Zanichelli, Bologna, Italy, 1969.
- ⁸Caputo, M., "Vibrations of an Infinite Plate with a Frequency Independent Q ," *Journal of the Acoustical Society of America*, Vol. 60, No. 3, Sept. 1976, p. 637.
- ⁹Caputo, M. and Minardi, F., *Pure and Applied Geophysics*, Vol. 91, 1971, pp. 134-147.
- ¹⁰Bagley, R. L., "Fractional Derivative Models for a Family of Corning Glasses," Technical report to be published by Air Force Wright Aeronautical Laboratories.
- ¹¹Bagley, R. L. and Torvik, P. J., "A Theoretical Basis for the Application of Fractional Calculus to Viscoelasticity," to be published in *Journal of Rheology*.
- ¹²Graves, G., Cannon, C., and Kumar, B., "A Study to Determine the Effect of Glass Compositional Variations on Vibration Damping Properties," Air Force Wright Aeronautical Laboratories, TR-80-4061, May 1980.
- ¹³Jones, D. I. G., "Viscoelastic Materials for Damping Applications," *Damping Applications for Vibration Control*, edited by P. J. Torvik, ASME, New York, 1980, pp. 27-51.
- ¹⁴Zienkiewicz, O. C., *The Finite Element Method in Structural and Continuum Mechanics*, McGraw-Hill Book Co., London, 1967, p. 220.
- ¹⁵Christensen, R. M., *Theory of Viscoelasticity, An Introduction*, Academic Press, New York, 1971, pp. 207-218.
- ¹⁶Foss, K. A., "Co-ordinates Which Uncouple the Equations of Motion of Damped Linear Dynamic Systems," *Journal of Applied Mechanics*, Vol. 25, Sept. 1958, p. 361.

AIAA Meetings of Interest to Journal Readers*

Date	Meeting (Issue of AIAA Bulletin in which program will appear)	Location	Call for Papers†
1983			
May 2-4	AIAA/ASME/ASCE/AHS 24th Structures, Structural Dynamics & Materials Conference (Mar.)	Sahara Hotel Lake Tahoe, Nev.	June 82
May 10-12	AIAA Annual Meeting and Technical Display (Aerospace Engineering Show) (Apr.)	Long Beach Convention Center Long Beach, Calif.	
June 1-3	AIAA 18th Thermophysics Conference (Apr.)	The Queen Elizabeth Hotel, Montreal, Quebec, Canada	Sept. 82
June 27-29	AIAA/SAE/ASME 19th Joint Propulsion Conference and Technical Display (Apr.)	Westin Hotel Seattle, Wash.	Sept. 82
July 12-14	AIAA 16th Fluid and Plasma Dynamics Conference (May)	Radisson Ferncroft Hotel and Country Club, Danvers, Mass.	Oct. 82
July 13-15	AIAA 6th Computational Fluid Dynamics Conference (May)	Radisson Ferncroft Hotel and Country Club, Danvers, Mass.	Oct. 82
July 13-15	AIAA Applied Aerodynamics Conference (May)	Radisson Ferncroft Hotel and Country Club, Danvers, Mass.	Oct. 82

*For a complete listing of AIAA meetings, see the current issue of the AIAA Bulletin.

†Issue of AIAA Bulletin in which Call for Papers appeared.